

## N O T I C E

THIS DOCUMENT HAS BEEN REPRODUCED FROM  
MICROFICHE. ALTHOUGH IT IS RECOGNIZED THAT  
CERTAIN PORTIONS ARE ILLEGIBLE, IT IS BEING RELEASED  
IN THE INTEREST OF MAKING AVAILABLE AS MUCH  
INFORMATION AS POSSIBLE

NASA Technical Memorandum 81607

## Fracture Toughness of Brittle Materials Determined With Chevron Notch Specimens

(NASA-TM-81607) FRACTURE TOUGHNESS OF  
BRITTLE MATERIALS DETERMINED WITH CHEVRON  
NOTCH SPECIMENS (NASA) 17 p HC A02/MF A01

N80-32486

CSCS 11F

Unclass

G3/26 28916

J. L. Shannon, Jr. and R. T. Bubsey

*Lewis Research Center*

and

D. Munz

*Universität Karlsruhe and Kernforschungszentrum Karlsruhe*

*Karlsruhe, FR Germany*

and

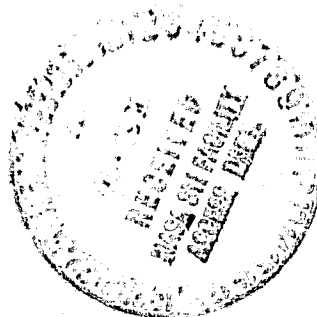
W. S. Pierce

*Lewis Research Center*

*Cleveland, Ohio*

Prepared for the  
Fifth International Conference on Fracture  
sponsored by the International Congress on Fracture  
Cannes, France, March 29-April 3, 1981

**NASA**



# FRACTURE TOUGHNESS OF BRITTLE MATERIALS DETERMINED WITH CHEVRON NOTCH SPECIMENS

J. L. Shannon, Jr.\*, R. T. Bubsey\*, D. Munz\*\* and W. S. Pierce\*

## INTRODUCTION

Increasing world-wide energy consumption has stimulated activity in the fields of coal and oil extraction and in energy conversion and usage systems such as coal gasifiers and high-temperature gas turbine engines. The role of fracture mechanics in these fields has grown, pointing to the specific need for standard test methods for determining the plane strain fracture toughness  $K_{Ic}$  of brittle non-metallic materials, principally rocks and ceramics.

Current fracture tests make use of a variety of specimen types (single edge bend, double torsion, double cantilever bend, and surface flawed specimens) having either blunt notches produced by saw cutting, or cracks produced by wedge loading, indenting, or local thermal shock. Specimens with blunt notches can overestimate  $K_{Ic}$ . Precracked specimens are difficult to prepare in a reproducible manner, and the initial crack front often cannot be seen on the fracture surface after testing, making it nearly impossible to measure the initial crack length. These current difficulties can be overcome by using a specimen containing a chevron notch in which a crack originates at the tip of the triangular ligament during loading. Specimens with a chevron notch were first used by Nakayama [1] in work of fracture studies, and later by Tattersall and Tappin [2] for fracture surface energy measurements. More recently, Barker [3] has proposed a chevron-notch specimen for plane strain fracture toughness measurement. The essential features of the chevron-notch specimen are that (1) a sharp natural crack is produced during the early stage of test loading (no precracking is required) and (2) the load passes through a maximum at a constant material-independent crack length-to-width ratio for a specific specimen geometry (no post-test crack length measurement is required). For materials with flat crack growth resistance curves, the plane strain fracture toughness  $K_{Ic}^*$  is proportional to the maximum test load, and a function of the specimen geometry and elastic compliance.

A development program on three chevron-notch specimens (short bar, short rod, and four-point-bend (see Figure 1)) has been underway at the NASA-Lewis Research Center Cleveland, Ohio, U.S.A., for the past three years. Stress intensity factor coefficients have been developed, both analytically and experimentally, and fracture toughness measurements on  $\text{Si}_3\text{N}_4$  and  $\text{Al}_2\text{O}_3$  have been made to assess the performance of each specimen type. Due to page limitations in this volume, only the short bar configuration will be treated in this paper. Results for the other two configurations may be found in references [4] through [7].

## STRESS INTENSITY FACTOR

The chevron notch (Figure 1) is characterized by the notch length at the specimen surface,  $a_1$ ; the notch length to the tip of the chevron,  $a_0$ ; and the specimen width,  $W$ , and thickness,  $B$ . The shaded areas in Figure 1 represent cracks of length  $a$ . The crack front length  $b$  is

$$b = B \frac{a - a_0}{a_1 - a_0} = B \frac{\alpha - \alpha_0}{\alpha_1 - \alpha_0} \quad (1)$$

where  $\alpha = a/W$ ,  $\alpha_0 = a_0/W$ , and  $\alpha_1 = a_1/W$

\*NASA-Lewis Research Center, Cleveland, Ohio, 44135, U.S.A.

\*\*Universität Karlsruhe and Kernforschungszentrum Karlsruhe, Karlsruhe, FR Germany

The relation between maximum load  $P_{\max}$  and fracture toughness  $K_{IC}^*$  is obtained by equating the available and the necessary energies for crack propagation. The energy available to extend the crack a small increment  $\Delta a$  is

$$\Delta U = \frac{P^2}{2W} \cdot \frac{dC_{tr}}{d\alpha} \cdot \Delta a \quad (2)$$

where  $C_{tr}$  is the elastic compliance of the chevron-notch specimen; the subscript "tr" denoting the fact that in the chevron-notch specimen, the crack proceeds through the chevron notch such that the two together constitute a discontinuity with a trapezoidal front. The energy necessary to extend the crack by the increment  $\Delta a$  is

$$\Delta \bar{W} = G_{IC} \cdot b \cdot \Delta a = \frac{K_{IC}^2}{E'} \cdot b \cdot \Delta a \quad (3)$$

with elastic modulus  $E' = E$  for plane stress and  $E' = E/(1-\nu^2)$  for plane strain.\*\*

During crack extension,  $\Delta U = \Delta \bar{W}$ , leading to

$$K_{IC} = P \left[ \frac{(dC_{tr}/d\alpha)E'}{2Wb} \right]^{1/2} = \frac{P}{B\sqrt{W}} \left[ \frac{1}{2} \cdot \frac{dC_{tr}}{d\alpha} \cdot \frac{\alpha_1 - \alpha_0}{\alpha - \alpha_0} \right]^{1/2} \quad (4)$$

where  $C_{tr}^I = E'BC_{tr}$  is the dimensionless compliance. The term

$$Y^* = \left[ \frac{1}{2} \cdot \frac{dC_{tr}^I}{d\alpha} \cdot \frac{\alpha_1 - \alpha_0}{\alpha - \alpha_0} \right]^{1/2} \quad (5)$$

is the dimensionless stress intensity factor coefficient. Maximum load occurs at the minimum of the term in brackets, and is designated  $Y_m^*$ .

\*The authors recognize that the designation  $K_{IC}$  is customarily reserved for that value of plane strain fracture toughness determined in strict accordance with the ANSI/ASTM E-399 Standard Test Method for Plane - Strain Fracture Toughness of Metallic Materials. However, for materials with flat crack growth resistance curves (i.e., extremely brittle materials), we believe the chevron-notch specimen would yield a plane strain fracture toughness value fully equivalent to  $K_{IC}$  of the E-399 test, and without the encumbrances of post-test crack length measurement and secant-line construction on the test record; therefore, the toughness values obtained in this investigation are designated  $K_{IC}$ .

\*\*There is some uncertainty about the usage of the plane strain or plane stress relation when stress intensity factors are derived from compliance measurements [8]. Whereas there is plane strain in the immediate vicinity of the notch at mid thickness, the bulk of the specimen is nearer the plane stress state. Therefore, Brown and Srawley [9] have proposed to omit the  $(1-\nu^2)$  term for  $E'$ .

There are no available analytical solutions for the chevron-notch short bar specimen stress intensity factor coefficient. However, as a first approximation it can be assumed that  $dC'_{tr}/d\alpha$  for the chevron notch with a crack is identical to that  $dC/d\alpha$  for a straight-through crack. This approximation is referred to as the "straight-through crack assumption", STCA. Using the relation for a straight-through crack

$$\frac{dC}{d\alpha} = 2Y^2 \quad (6)$$

where

$$Y = \frac{KB\sqrt{W}}{P},$$

Eqs. (4) and (5) can be rewritten

$$K_{Ic} = \frac{P}{B\sqrt{W}} Y \left[ \frac{\alpha_1 - \alpha_0}{\alpha - \alpha_0} \right]^{1/2} \quad (7)$$

and

$$Y^* = Y \left[ \frac{\alpha_1 - \alpha_0}{\alpha - \alpha_0} \right]^{1/2} \quad (8)$$

where  $Y^*$  is the chevron-notch and  $Y$  the straight-through crack specimen coefficients.

The dimensionless stress intensity factor coefficient for the short bar specimen with a straight-through crack is [10]:

$$Y = \frac{\alpha}{(1-\alpha)^{3/2}} \ln \left( \exp \left[ \frac{2.702}{\alpha} + 1.628 \right] + \exp \left\{ \left[ 12 \frac{W^3 (1-\alpha)^3}{H^3} \right]^{1/2} \left[ 1 + \frac{0.679}{\alpha(W/H)} \right] \right\} \right) \quad (9)$$

To check the validity of the straight-through crack assumption, a series of short bar experimental compliance measurements were made [10]. The compliance specimens were machined in the L-T crack plane orientation from 7075-T651 aluminum plate to the dimensions shown in Figure 2a for  $W/H$  ratios of 3 and 4. A 17.8 mm slot was machined into the front face to accommodate loading knife edges (Figure 2b). The displacements measurements were made with a modified ASTM E-399 clip-in gage as shown in Figure 2c. Hardened steel cones were fastened to the inner surfaces of the displacement gage arms and set into small indentations in the top and bottom of the specimens [6]. A 0.6 mm slot was extended incrementally to simulate an advancing crack in the specimen.

The compliance results for specimen proportioned  $W/H = 4$  are presented as functions of the notch parameters  $\alpha_0$  in Figures 3 and  $\alpha_1$  in Figure 4. The results for specimen proportioned  $W/H = 3$  were, of course, quite similar. The compliance curves were differentiated to obtain  $dC'_{tr}/d\alpha$  for substitution into Eq. (5)

for the stress intensity factor coefficient  $Y^*$ .  $Y^*$ 's obtained in this way from Figure 3 are compared in Figure 5 with  $Y^*$ 's obtained analytically using the STCA relation of Eqs. (8) and (9).

In the region of the curve minima, designated  $Y_m^*$  and indicated by arrows to the curves, the experimental and analytical results agree extraordinarily well: less than 4 percent difference for the greatest initial crack length ( $\alpha_0=0.495$ ), and less than 1 percent difference for the two shorter initial crack lengths. As expected, the minima decrease and broaden with decreasing  $\alpha_0$ . Location of the minima at  $\alpha_m$  corresponding to maximum load (and  $Y_m^*$ ) varies in such a way that the quantity  $(\alpha_m - \alpha_0)$ , which is the relative crack extension up to maximum load, passes through a maximum as shown in Figure 6.

Experimental results showing the influence of  $\alpha_1$  on  $Y^*$  are shown in Figure 7. Decreasing  $\alpha_1$  lowers the curves and, at  $\alpha = \alpha_1$ , the chevron-notch specimen curves join the curve for a straight-through crack specimen. According to the straight-through crack assumption, the location of the curve minima should not vary; e.i. the relative crack length at maximum load  $\alpha_m$  should be independent of  $\alpha_1$  (shown by differentiating Eq. (8) with respect to  $\alpha$  for  $\alpha = \alpha_m$ ). Experimentally, however,  $\alpha_m$  will vary with  $\alpha_1$ , and this too is predictable from the differentiation of Eq. (8). This dependence of  $\alpha_m$  on  $\alpha_1$  produces a continuous rise in the amount of relative crack extension up to maximum load  $(\alpha_m - \alpha_0)$  as a function of  $\alpha_1$  as shown in Figure 8.

The minimum values  $Y_m^*$  of  $Y^*$  are used in conjunction with  $P_{max}$  to compute  $K_{Ic}$ . Since no practical difference was observed between the experimental and analytical  $Y_m^*$  values, and for the sake of computational simplicity, the STCA values were used for all  $K_{Ic}$  calculations in the toughness measurements portion of this study. Under the STCA,  $K_{Ic}$  for the short bar specimen may be expressed:

$$K_{Ic} = \frac{P}{B\sqrt{W}} Y^* \quad (10)$$

Substituting  $P_{max}$  for  $P$  and  $Y_m^*$  for  $Y^*$ ,  $K_{Ic}$  is obtained from maximum load with no need for crack length measurement. For specimens with  $\alpha_1 = 1$ , and in the range  $3 \leq W/H \leq 4$  and  $0.2 \leq \alpha_0 \leq 0.5$ ,  $Y_m^*$  may be expressed:

$$Y_m^* = \left[ 4.08 + 3.95 \left( \frac{W}{H} \right) + 0.50 \left( \frac{W}{H} \right)^2 + \left[ -23.15 + 1.15 \left( \frac{W}{H} \right) + 1.30 \left( \frac{W}{H} \right)^2 \right] \alpha_0 \right. \\ \left. + \left[ 172.5 - 43.5 \left( \frac{W}{H} \right) + 3.0 \left( \frac{W}{H} \right)^2 \right] \alpha_0^2 \right] \quad (11)$$

This equation is in agreement with the analytical  $Y_m^*$  from Eq. (8), within  $\pm 0.3\%$ . For  $\alpha_1 < 1$ , Eq.(11) must be multiplied by  $\left[ (\alpha_1 - \alpha_0)/(1 - \alpha_0) \right]^{1/2}$ .

#### FRACTURE TOUGHNESS MEASUREMENTS

Two materials were investigated: Norton Company NC-132 hot pressed silicon nitride ( $\text{Si}_3\text{N}_4$ ) and 3M Company Alsimag-614 sintered aluminum oxide ( $\text{Al}_2\text{O}_3$ ). The  $\text{Si}_3\text{N}_4$  was acquired as 150 mm x 150 mm x 10 mm thick plate; the  $\text{Al}_2\text{O}_3$  as bars 12.7 mm x 12.7 mm x 29.2 mm and 25.4 mm x 25.4 mm x 54.6 mm. Short bar specimens were machined to the dimensions shown in Figure 9. Chevron notches were produced by diamond-impregnated wire sawing or by diamond wheel slotting. Details regarding specimen preparation and test procedure have been given in reference [11].

## RESULTS

The plane strain fracture toughness of  $\text{Si}_3\text{N}_4$  determined with short bar specimens of  $\alpha_1 = 1.0$  and  $0.17 \leq \alpha_0 \leq 0.48$  is plotted in Figure 10. A value of  $K_{IC}$  equal to  $4.64 + 0.11 \text{ MNm}^{-3/2}$  appears well established and independent of the dimension  $\alpha_0$ . The limited amount of data shown in Figure 11 for specimens with  $\alpha_0 = 0.20$  and  $0.50 \leq \alpha_1 \leq 0.99$  suggests independence of  $K_{IC}$  on  $\alpha_1$  as well, and substantiates the mean  $K_{IC}$  value obtained from the data of Figure 10.

The aluminum oxide chevron-notch short bar specimen geometries varied in  $\alpha_0$ ,  $\alpha_1$ , W/H and absolute size (see Figure 9). Plane strain fracture toughness results are shown in Figures 12 and 13. For chevron notches with  $\alpha_1 = 1$ , there is a small downward trend in  $K_{IC}$  with increasing initial relative crack length  $\alpha_0$  (Figure 12). Over the range investigated, this effect is less than 4 percent. A more interesting feature is the strong dependence of  $K_{IC}$  on specimen thickness and width-to-half height ratio. Comparing mean values of  $K_{IC}$ , the thickness effect appears about double that of the W/H ratio. The results for W/H = 4 exceed those for W/H = 3 by 6 percent for B = 25.4 mm and by 10 percent for B = 12.7 mm. The results for B = 25.4 mm exceed those for B = 12.7 mm by 15 percent for W/H = 4 and by 18 percent for W/H = 3.

The largest effect was produced by variation in the relative length of the chevron notch at the specimen surface,  $\alpha_1$  (Figure 13).  $K_{IC}$  drops nearly 25 percent with decreasing  $\alpha_1$  in the range investigated.

## PRACTICAL SIGNIFICANCE OF RESULTS

Implicit in the STCA, and underlying the theoretical base for the chevron notch specimen, is the presumption of a flat crack growth resistance curve for the material tested. When this condition is not met, the chevron-notch specimen will yield  $K_{IC}$  values which vary with specimen geometry and size, and therefore is of questionable usefulness in its present state of development. It would appear that the  $\text{Si}_3\text{N}_4$  tested in this program does satisfy the requirement of a flat crack growth resistance curve and therefore demonstrates the usefulness of the chevron-notch short bar specimen for plane strain fracture toughness evaluation of this material.

In contrast, the  $\text{Al}_2\text{O}_3$  material appears to have a rising crack growth resistance curve, as evidenced by the size and geometry dependence of its measured  $K_{IC}$ . Since  $K_{IC}$  is calculated from maximum load, its value will depend on the amount of crack extension up to maximum load, and this will vary with chevron notch geometry (see Figures 6 and 8), specimen size, and specimen proportions, W/H. The effect is to vary the point on the rising crack growth resistance curve at which maximum load occurs. Dependence of the notch parameters  $\alpha_0$  and  $\alpha_1$  on the amount of crack growth up to maximum load for the two series of  $\text{Al}_2\text{O}_3$  specimens in Figures 12 and 13, is shown in corresponding Figures 6 and 8. The results of Figure 12 wherein  $\alpha_0$  is the controlling chevron notch parameter are plotted in Figure 14 in terms of the crack extension up to maximum load, and provide in effect a gradually rising crack growth resistance curve. A similar exercise involving the data of Figure 13 ( $\alpha_1$  variable) results in the plot of Figure 15. Surprisingly, the curve of Figure 15, reflecting change in  $\alpha_1$ , is much steeper than that of Figure 14 for change in  $\alpha_0$ . At this juncture, the authors can offer no explanation for this difference, but clearly the basic effect is due to a rising crack growth resistance curve for the  $\text{Al}_2\text{O}_3$  material tested.

The range of  $\alpha_0$ 's investigated was for each specimen size and proportions tested, in the segment of negative slope of the  $(\alpha_m - \alpha_0)$  vs  $\alpha_0$  curves of Figure 6. It would appear that the slight downward trend of  $K_{IC}$  with increasing

$\alpha_0$  in Figure 12 is due to this effect, although it is surprisingly small compared to the  $\alpha_1$  effect in Figure 13 which is due to no greater trend in  $(\alpha_m - \alpha_0)$  vs  $\alpha_1$  in Figure 8.

The authors feel the results of this investigation are precautionary in the use of the chevron notch specimen for materials with rising crack growth resistance curves. Tests of any material for its plane strain fracture toughness cannot be considered conclusive unless specimens of more than one geometry and/or size give the same result.

It would appear also from the results that there is a preferred chevron geometry; namely,  $\alpha_0 = 0.2$  and  $\alpha_1 = 1.0$ . These correspond to the maximum amount of crack extension up to maximum load, and therefore should provide the greatest stability of the crack front at the measurement point. This would also provide for the greatest sensitivity to non-flat crack growth resistance curves, and be most selective in applicability of the test, which at this time must be restricted to flat crack growth resistance-type materials.

#### REFERENCES

1. J. Nakayama, "Direct Measurement of Fracture Energies of Brittle Heterogeneous Materials", J. Am. Ceram. Soc., 48:11 (1965), pp.583-587.
2. H. G. Tattersall and G. Tappin, "The Work of Fracture and Its Measurement in Metals, Ceramics and other Materials", J. Mater. Sci., 1:3 (1966), pp.296-301.
3. L. M. Barker, "A Simplified Method for Measuring Plane Strain Fracture Toughness", Eng. Fracture Mech., 9:2 (1977) pp. 361-369.
4. D. Munz, R. T. Bubsey, and J. L. Shannon, Jr., "Fracture Toughness Determination of  $Al_2O_3$  Using Four-Point-Bend Specimens with Straight-Through and Chevron Notches", J. Am. Ceram. Soc., 63:5-6 (1980), pp. 300-305.
5. D. Munz, J. L. Shannon, Jr. and R. T. Bubsey, "Fracture Toughness Calculation from Maximum Load in Four Point Bend Tests of Chevron Notch Specimens", to be published in Int. J. Fracture.
6. R. T. Bubsey, D. Munz, W. S. Pierce, and J. L. Shannon, Jr., "Compliance Calibration of the Short Rod Chevron-Notch Specimen for Fracture Toughness Testing of Brittle Materials", to be published in Int. J. Fracture.
7. Paper on plane strain fracture toughness determinations on  $Al_2O_3$  using the short rod chevron-notch specimen in preparation.
8. R. T. Bubsey, D. M. Fisher, M. H. Jones and J. E. Srawley, "Compliance Measurements", Experimental Techniques in Fracture Mechanics, S.E.S.A. Monograph 1, A. S. Kobayashi, ed., Iowa State Univ. Press and Society for Experimental Stress Analysis, Cambridge (1976), pp. 76-95.
9. W. F. Brown, Jr. and J. E. Srawley, Plane Strain Crack Toughness Testing of High Strength Metallic Materials, ASTM STP 410, Am. Soc. for Testing & Materials, Philadelphia (1967).
10. D. Munz, R. T. Bubsey, and J. E. Srawley, "Compliance and Stress Intensity Coefficients for Short Bar Specimens with Chevron Notches", Int. J. Fracture, 16:4 (1980), pp. 359-374.



11. D. Munz, R. T. Bubsey, and J. L. Shannon, Jr., "Performance of Chevron-Notch Short Bar Specimen in Determining the Fracture Toughness of Silicon Nitride and Aluminum Oxide", J. Test. Eval., 8:3 (1980), pp. 103-107.

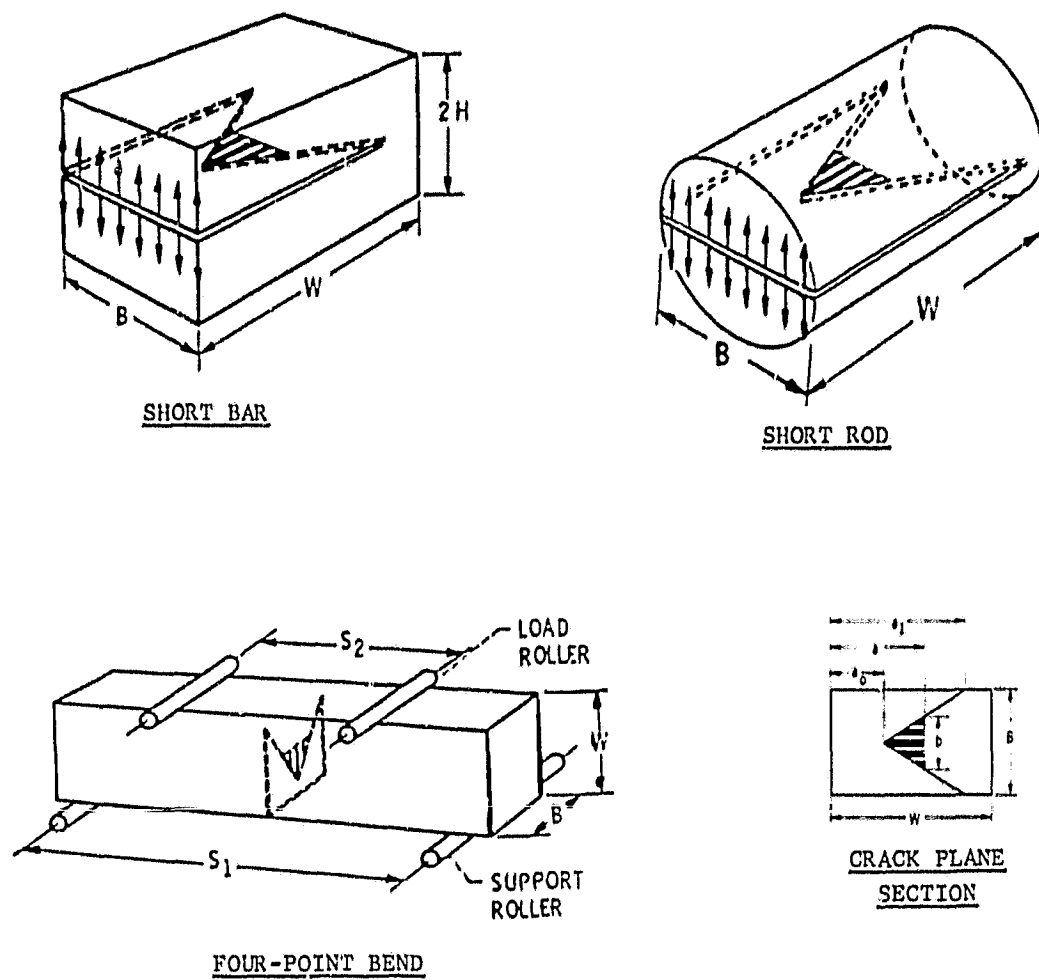


Figure 1. - Chevron-notch specimens.

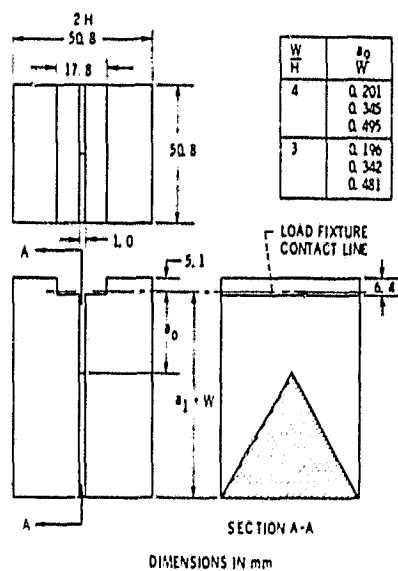


Figure 2a. - Short bar chevron-notch compliance specimen.

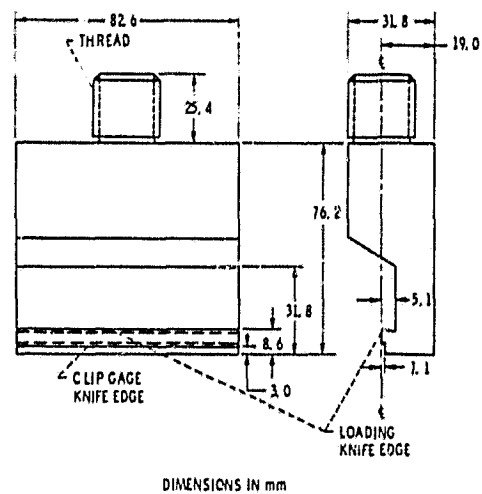


Figure 2b. - Loading fixture.

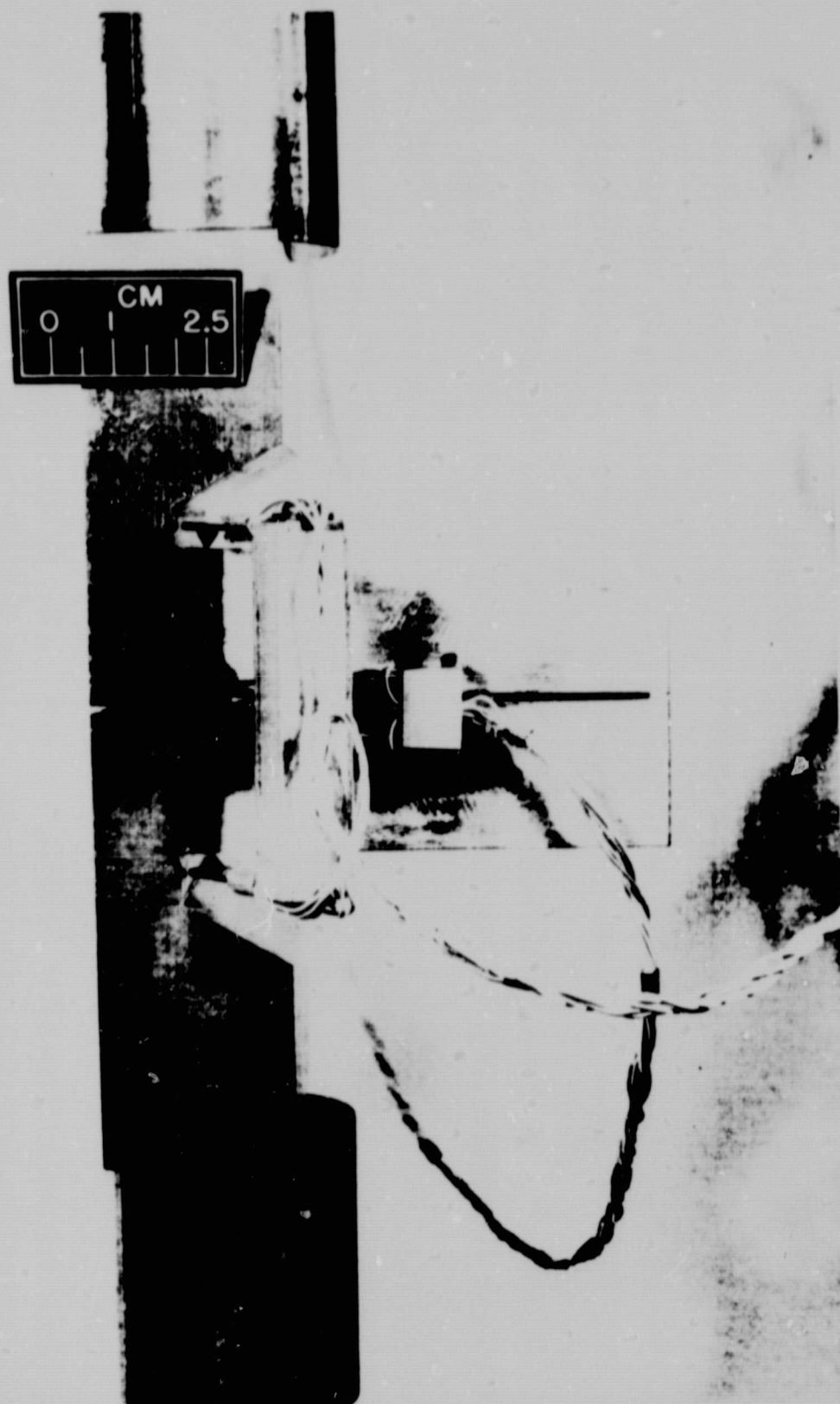


Figure 2c. - Crack mouth opening displacement gage fastened to short bar chevron-notch compliance specimen mounted in loading fixture.

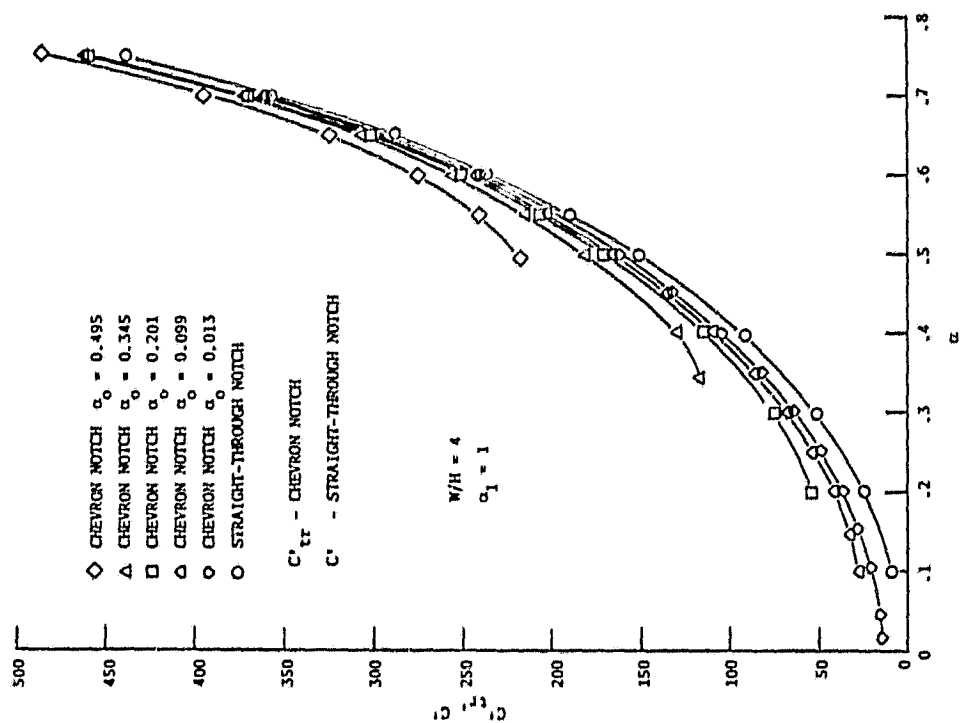


Figure 3. - Effect of  $a$  on dimensionless compliance for short bar specimens of  $W/H = 4$  proportions with either a straight-through notch or chevron notches of  $\alpha_1 = 1$  and various  $\alpha_0$ .

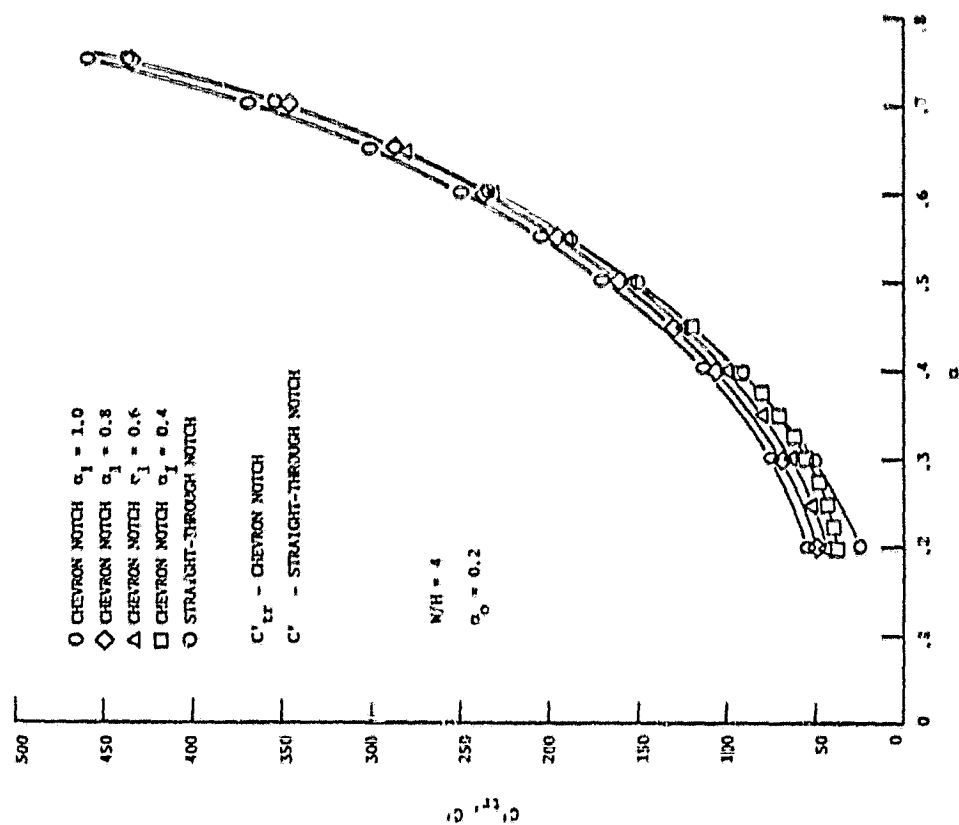


Figure 4. - Effect of  $a$  on dimensionless compliance for short bar specimens of  $W/H = 4$  proportions with either a straight-through notch or chevron notches of  $\alpha_0 = 0.2$  and various  $\alpha_1$ .

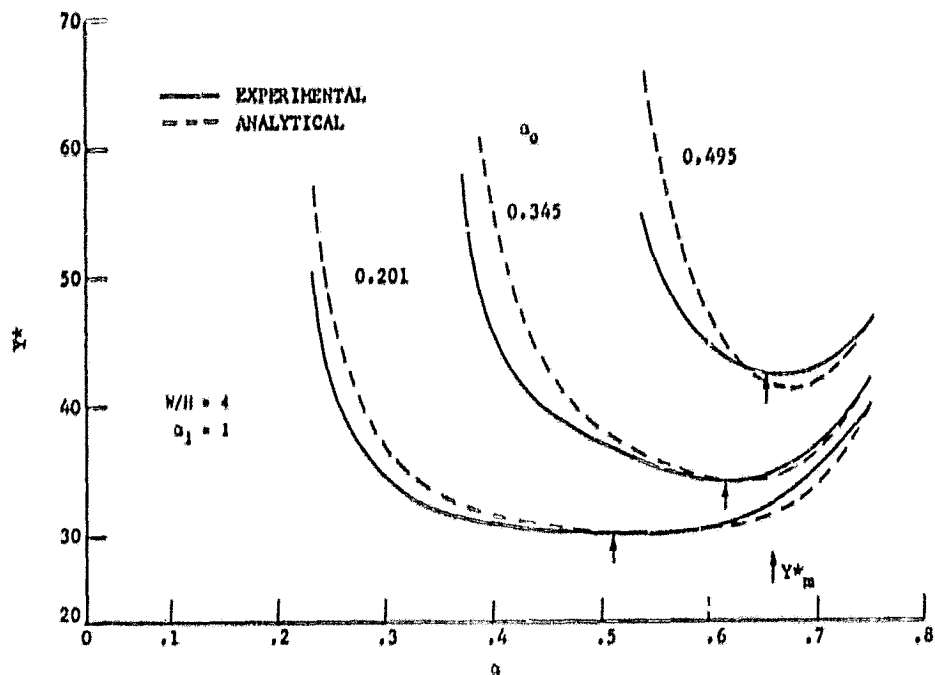


Figure 5. - Stress Intensity factor coefficient  $Y^*$  determined experimentally and analytically for short bar chevron-notch specimens of  $W/H = 4$ ,  $\alpha_1 = 1$ , and various  $\alpha_0$ .

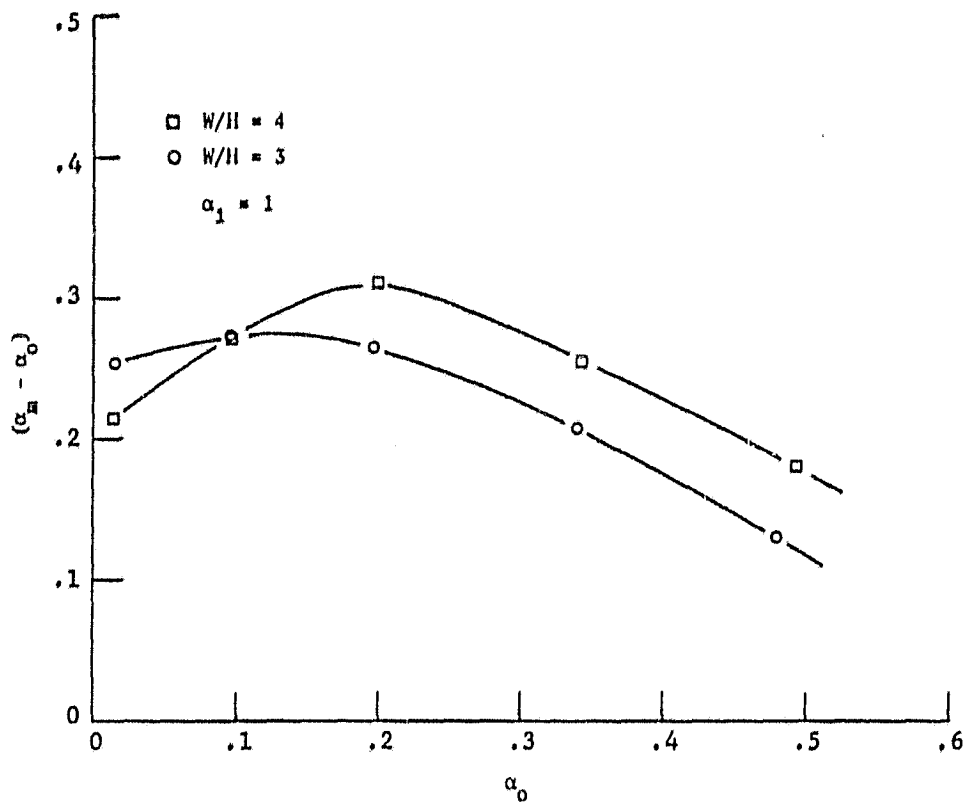


Figure 6. - Relative crack extension  $(\alpha_m - \alpha_0)$  at the minimum value of  $Y^*$  as a function of  $\alpha_0$  for short bar chevron-notch specimens of  $W/H = 3$  and  $4$  and  $\alpha_1 = 1$ .

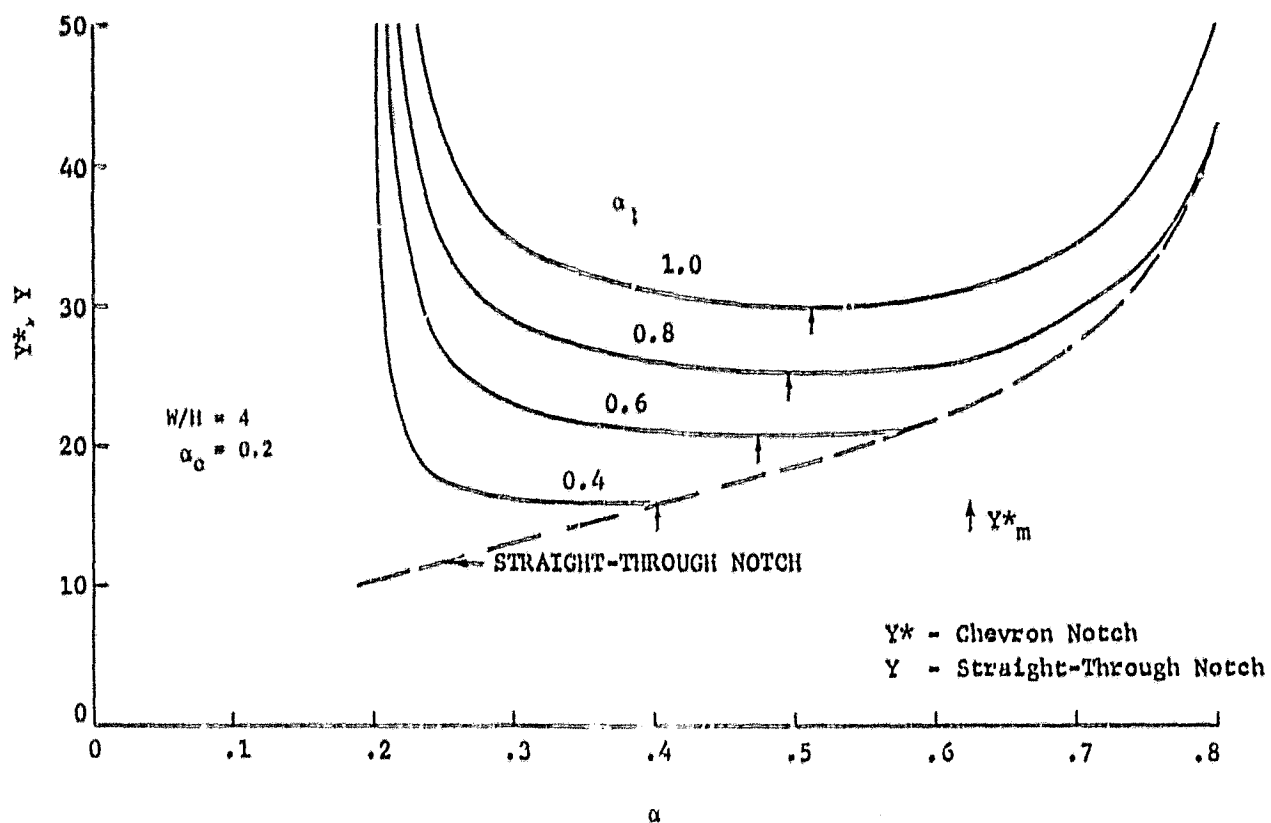


Figure 7. - Experimentally determined stress intensity factor coefficient for short bar specimens of  $W/H = 4$  containing either a chevron notch of  $\alpha_0 = 0.2$  or a straight-through notch.

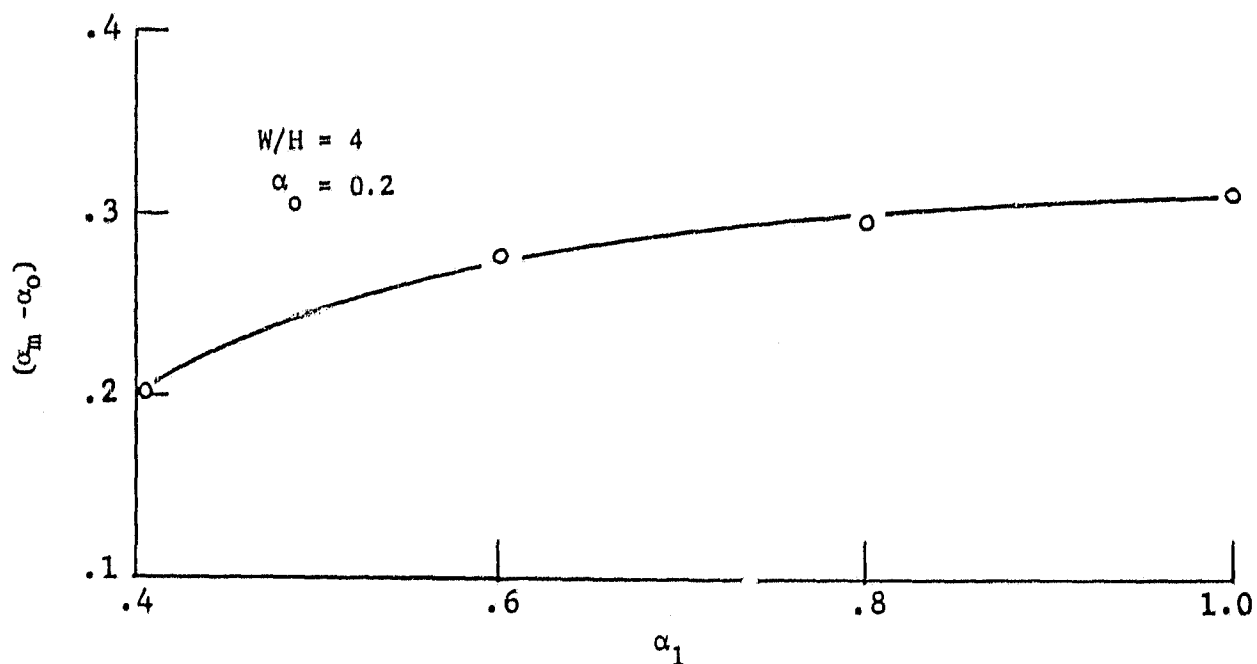
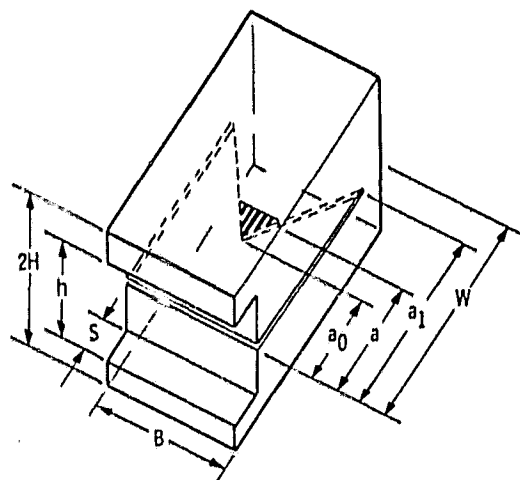


Figure 8. - Relative crack extension  $(\alpha_m - \alpha_0)$  at the minimum value of  $Y^*$  as a function of  $\alpha_1$  for short bar chevron-notch specimens of  $W/H = 4$  and  $\alpha_0 = 0.2$ .



MATERIAL	B	W	H	W/H	h	S	$a_0$	$a_1$
$Si_3N_4$	8.8 - 9.6	15.2	4.5	3.4	6.3	2.5	2.5 - 7.3	7.5 - 15.2
$Al_2O_3$	25.4	50.8	12.7	4.0	12.7	3.8	10.6 - 22.2	50.8
	25.4	38.1	12.7	3.0	12.7	3.8	8.6 - 17.6	38.1
	12.7	25.4	6.35	4.0	6.3	3.8	4.9 - 11.5	10.2 - 25.4
	12.7	19.1	6.35	3.0	6.3	3.8	1.7 - 6.9	19.1

ALL DIMENSIONS IN mm.

Figure 9.—Chevron-notch short bar fracture toughness test specimen.

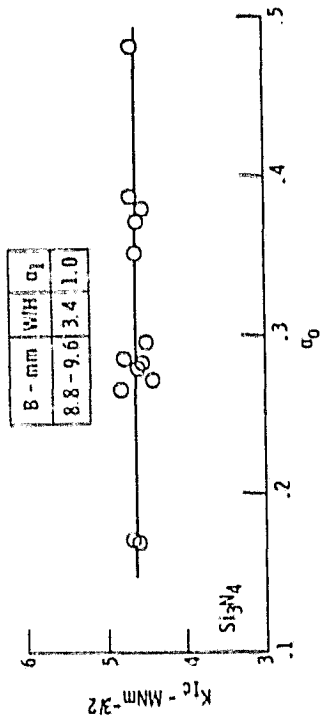


Figure 10. Effect of  $\sigma_0$  on  $K_{IC}$  of hot pressed silicon nitride MC-130 determined with chevron-notch short bar specimens.

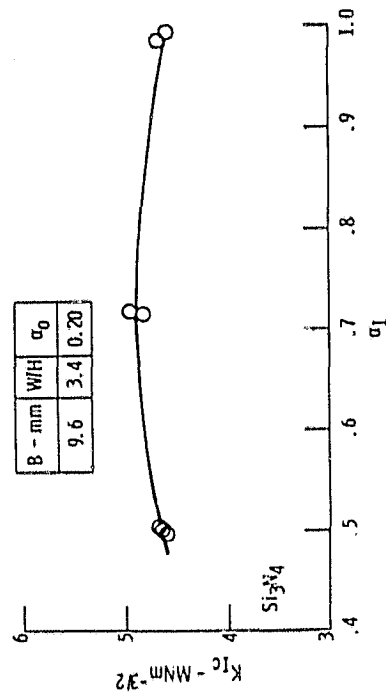


Figure 11. Effect of  $\sigma_1$  on  $K_{IC}$  of hot pressed silicon nitride MC-130, determined with chevron-notch short bar specimens.

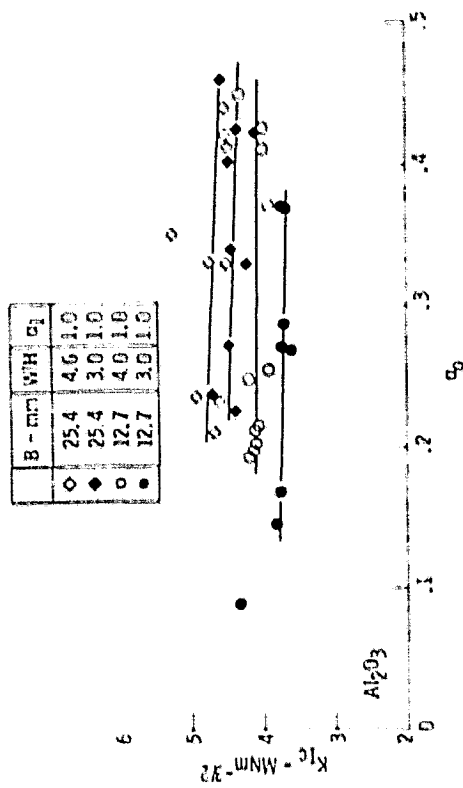


Figure 12. Effect of  $\sigma_0$  on  $K_{IC}$  of sintered aluminum oxide Alomag-614 determined with chevron-notch short bar specimens.

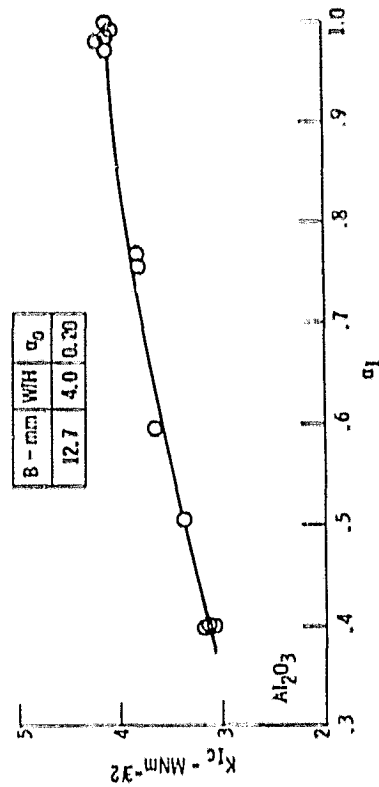


Figure 13. Effect of  $\sigma_1$  on  $K_{IC}$  of sintered aluminum oxide Alomag-614 determined with chevron-notch short bar specimens.



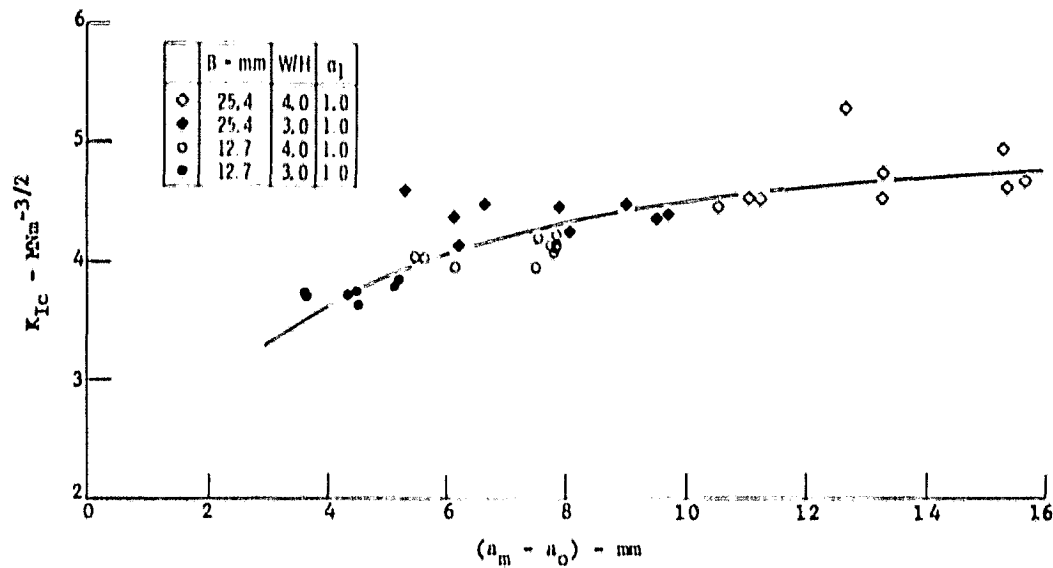


Figure 14. - Variation in  $K_{IC}$  of sintered aluminum oxide (Alsimag-614) with amount of crack extension up to maximum load for short bar chevron-notch specimens of  $a_1 = 1$  in two thicknesses and W/H proportions, and variable chevron notch angle as obtained by varying the initial crack length  $a_0$ .

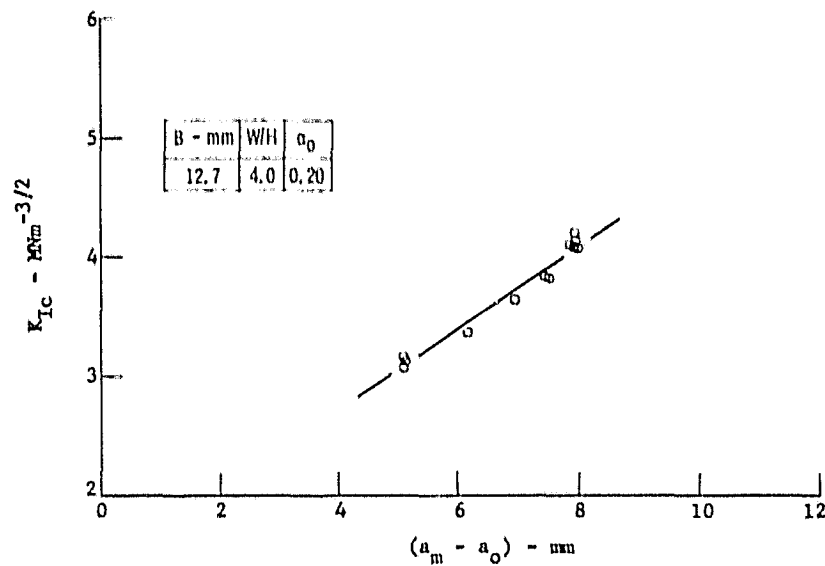


Figure 15. - Variation in  $K_{IC}$  of sintered aluminum oxide (Alsimag-614) with amount of crack extension up to maximum load for short bar chevron-notch specimens of W/H = 4,  $a_0 = 0.2$ , and variable chevron notch angle as obtained by varying  $a_1$ .